



Differential involvement of mitochondria during ursolic acid-induced apoptotic process in HaCaT and M4Beu cells

RAPHAËL EMMANUEL DUVAL^{1,4*}, PIERRE-OLIVIER HARMAND^{1,5*}, CHANTAL JAYAT-VIGNOLES²,
JEANNE COOK-MOREAU³, ALINE PINON¹, CHRISTIANE DELAGE¹ and ALAIN SIMON¹

¹EA 4021, Laboratoire de Chimie-Physique, Faculté de Pharmacie; ²UMR CNRS 6101, Faculté de Médecine;

³Laboratoire de Biochimie Médicale, Faculté de Médecine, 2 rue du Docteur Marcland, 87025 Limoges Cedex, France

Received May 25, 2007; Accepted August 3, 2007

Abstract. Ursolic acid (UA) is a pentacyclic triterpenoid compound which exists widely in nature and is known to have a pleiotropic biological activity profile. For the last few decades, extensive work has been carried out to establish its biological activities and pharmacological actions. It is described as a promising chemopreventive agent with an antiproliferative effect on cancer cells that stems from its ability to induce apoptosis. We investigated and compared the role played by mitochondria during the apoptotic process induced by UA in human HaCaT-derived keratinotic cells and M4Beu human melanoma cells. In both cell lines, UA induced significant caspase-3 activation, the downstream central effector of apoptosis. Subsequent JC-1/TOTO-3 double staining clearly demonstrated that UA induces strong mitochondrial-transmembrane potential collapse in M4Beu cells, while mitochondria from HaCaT-treated cells remain largely unstimulated. This was confirmed by Western blot analysis, which revealed a Bax/Bcl-2-balance change in favor of Bax, the proapoptotic member, in UA-treated M4Beu cells. It can be concluded that UA induces apoptosis in M4Beu through the mitochondrial pathway, while other mechanisms are activated in the case of HaCaT cells.

Introduction

Among natural compounds, ursolic acid (UA), the most frequently studied natural triterpenic acid (1), seems to be a promising chemical entity for the protection of human skin. Indeed, in cosmetology UA is often used for photoaging protection (2). It prevents and improves the appearance of wrinkles and age spots by restoring skin collagen structure and elasticity, stimulates collagen production in cultured fibroblasts and increases the production of ceramides in human epidermal keratinocytes and skin (3). UA may also be an effective inhibitor of the UVA-modulated signal transduction pathway in human HaCaT cells, in which it significantly suppresses UVA-induced reactive oxygen species production and lipid peroxidation (4). Moreover, it possesses anti-tumor properties including the inhibition of skin tumorigenesis (5) and tumor promotion (6). UA also induces apoptosis in several cancer cell lines (7-13).

Previously, we studied the effect of UA on human HaCaT-derived keratinotic cells and M4Beu human melanoma cells with the intention of confirming its role as a promising candidate for skin cancer prevention. In those studies, we demonstrated for the first time that UA has a significant antiproliferative effect associated with the induction of the apoptotic process (14,15). In the literature, it is well established that the activation of the apoptotic transduction pathway is dependent on cell type and subcellular targets. The two main apoptotic pathways are the extrinsic and intrinsic pathways (16). The extrinsic pathway is characterized by death ligand attachment on extracellular receptors (e.g. TNF/TNF-R) with a subsequent caspase-8 activation, which in turn cleaves and activates caspase-3 (17). The intrinsic pathway is triggered by different mitochondrial stresses and is characterized by mitochondrial transmembrane potential ($\Delta\psi_m$) collapse, closely regulated by Bcl-2 family members (18). Bax-like-proapoptotic members promote leakage of apoptogenic factors from the mitochondria, whereas Bcl-2-like-antiapoptotic members negatively regulate it (19).

With the aim of better understanding the proapoptotic effect of UA on immortalized HaCaT and melanoma M4Beu cells, we studied and compared the involvement of mitochondria in the apoptotic process induced by UA. Caspase-9 activity measurement suggested that the mitochondrial pathway was implicated in both cell lines.

Correspondence to: Dr Alain Simon, Laboratoire de Chimie-Physique, Faculté de Pharmacie, 2 rue du Docteur Marcland, 87025 Limoges Cedex, France
E-mail: simon@unilim.fr

Present addresses: ⁴GEVSM, UMR 7565, Nancy Université-CNRS, Faculté de Pharmacie, 5 rue Albert Lebrun, BP 80403, 54001 Nancy Cedex, France; ⁵Equipe Récepteurs Nucléaires et Transcription-Endocrinologie Moléculaire et Cellulaire des Cancers, INSERM U540, 60 rue de Navacelles, 34090 Montpellier, France

*Contributed equally

Key words: ursolic acid, HaCaT, M4Beu, apoptosis, mitochondria

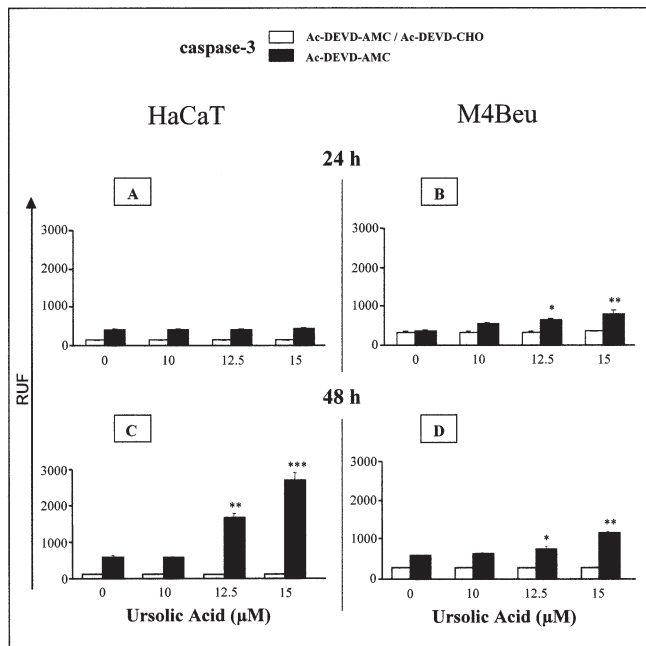


Figure 1. Effect of UA on caspase-3 activity in HaCaT and M4Beu cells. Caspase-3 activity was measured in the presence or absence of UA for 24 and 48 h. Filled bars represent caspase activity, stated in relative units of fluorescence without a specific inhibitor. Open bars correspond to caspase activity in the presence of caspase-specific inhibitor. Results are the mean \pm SD (* p <0.05; ** p <0.01; *** p <0.005) of three separate experiments.

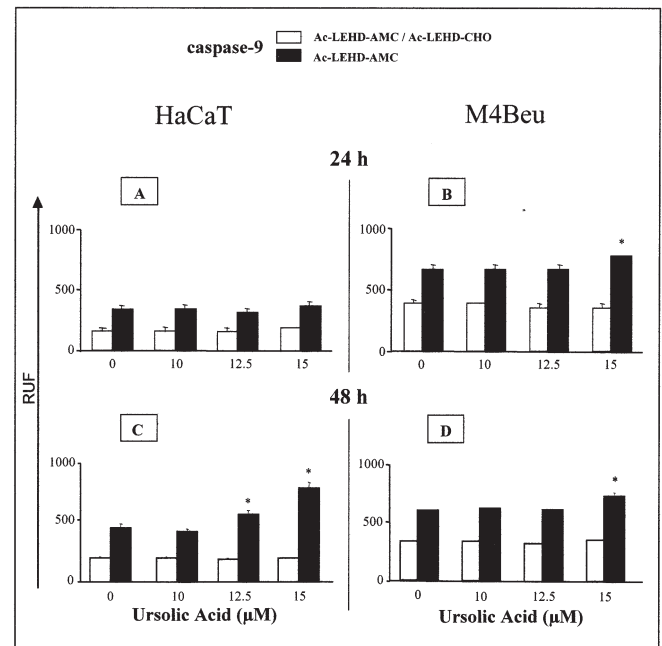


Figure 2. Effect of UA on caspase-9 activity in M4Beu cells. Caspase-9 activity was measured in the presence or absence of UA for 24 and 48 h. Filled bars represent caspase activity, stated in relative units of fluorescence without a specific inhibitor. Open bars correspond to caspase activity in the presence of caspase-specific inhibitor. Results are the mean \pm SD (* p <0.05; ** p <0.01) of three separate experiments.

Therefore, we performed JC-1/ TOTO-3 double staining to evaluate cell death according to $\Delta\psi_m$ and plasma membrane integrity changes. Combining these two probes resulted in a rapid and accurate discrimination between high and low mitochondrial polarizations. As $\Delta\psi_m$ is controlled by Bcl-2 family members, we also studied both proapoptotic Bax and antiapoptotic Bcl-2 proteins, which are the two major regulators of mitochondrial membrane permeabilization. In conclusion, our results clearly demonstrate a stronger UA-induced mitochondria-pathway triggering effect in M4Beu than in HaCaT cells.

Materials and methods

UA was purchased from Sigma (St. Quentin Fallavier, France). JC-1 (5,5',6,6'-tetrachloro-1,1',3,3'-tetraethylbenzimidazolyl-carbocyanine iodide; Invitrogen, Cergy Pontoise, France), was prepared in DMSO (100 μ g/ml) and used at a final solution of 1 μ g/ml. TOTO-3 {1,1-(4,4,8,8-tetramethyl-4,8-diazaundecamethylene)-bis-4-[3-methyl-2,3-dihydro-(benzo-1,3-thiazole)-2-methylidene]-quinolinium tetraiodide; Invitrogen}, was prepared in DMSO and used at a final solution of 1 μ M. Caspase-3 substrate AC-DEVD-AMC and inhibitor Ac-DEVD-CHO were provided by CaspACE Assay System Fluorometric (Promega, Charbonnières, France). Caspase-9 substrate AC-LEHD-AMC and inhibitor Ac-LEHD-CHO were provided by Bachem Biochimie (Voisins-le-Bretonneux, France).

Primary antibodies Bax (B9, sc-7480) and Bcl-2 (100, sc-509) were purchased from Santa-Cruz (Heidelberg, Germany) and β -Actin (AC-15) from Sigma. Secondary antibodies were purchased from Dako (Trappes, France).

Cell line, cell culture and treatment. HaCaT cells, a human-derived keratinocyte line, and M4Beu cells, a human melanoma cell line, were cultured in Dulbecco's modified Eagle's medium, 25 mM HEPES, and in Eagle's minimum essential medium, 25 mM HEPES, respectively. Both were supplemented with 10% foetal calf serum, 1% non-essential amino-acids (x100), 1% vitamins (x100), 1% L-glutamine (200 mM) and 0.2% gentamycin (10 mg/ml). All products were purchased from Gibco BRL, France. Cultures were maintained in a humidified atmosphere with 5% CO₂ at 37°C.

Detection of caspase catalytic activities. Caspase activities were analyzed using their specific substrates as previously described (15). Briefly, after incubation with UA for 24 or 48 h, cells were harvested, lysed and fluorometric assays were measured using 360 nm excitation and 460 nm emission. Raw data (relative unit of fluorescence or RUF) corresponded to the concentrations of AMC released.

JC-1 and TOTO-3 staining for flow cytometric analysis. Changes in mitochondrial membrane potential were estimated using fluorescent probes JC-1 and TOTO-3. JC-1 indicates mitochondrial polarization whereas TOTO-3, a membrane impermeant probe, enters cells with altered plasma membrane integrity, binds to nucleic acids and exhibits strong red fluorescence, enabling discrimination between intact and altered cells. After UA treatment or, in the case of the controls, medium alone, HaCaT and M4Beu cells were stained according to Zuliani *et al* (20). Briefly, suspensions were adjusted to 10⁶ cells/ml, stained for 35 min with 1 μ g/ml JC-1 at 37°C and then for 5 min with 1 μ M TOTO-3 at 37°C. Cells were analyzed by flow cytometry (FCM) immediately after staining.

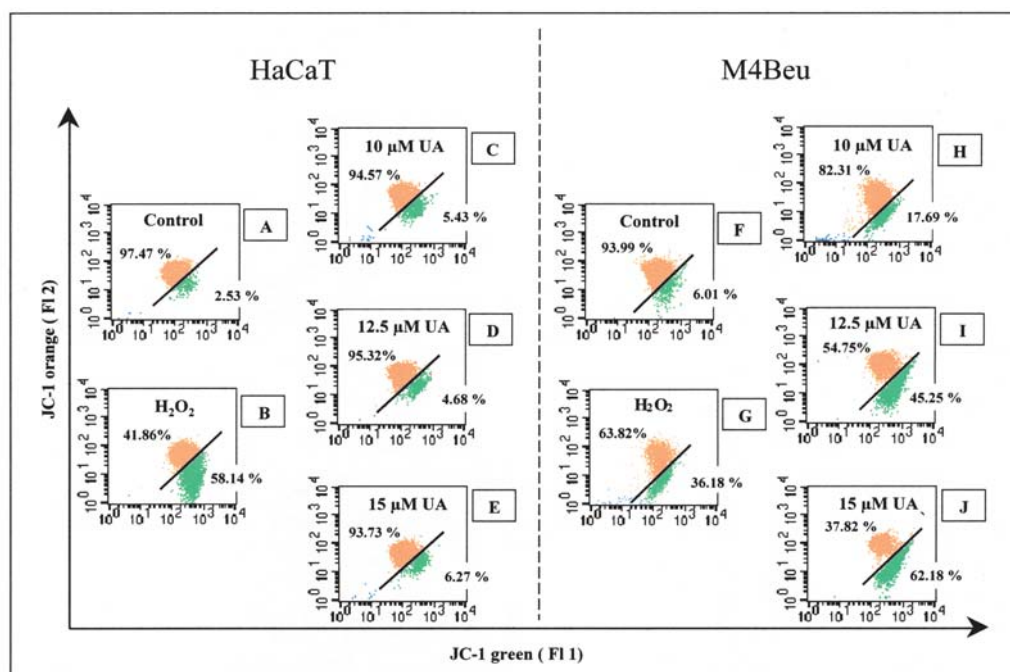


Figure 3. Cytometric analysis of $\Delta\psi_m$ collapse after UA treatment. HaCaT and M4Beu cells were incubated in the presence or absence of UA for 24 h. Cytograms were gated to quantify JC-1^{high} (orange) and/or low (green) mitochondrial potential in viable cells (TOTO-3⁻). Dead cells labeled by TOTO-3 (TOTO-3⁺) were excluded. Cytograms were typical of three independent experiments. Cells incubated with 1 mM H₂O₂ served as a positive control. F11, JC-1 green fluorescence; F12, JC-1 orange fluorescence.

Flow cytometric analysis. Analysis was performed on a FACS Vantage (Becton-Dickinson, USA) equipped with a 633 nm helium/neon laser (TOTO-3-excitation) and a 488 nm argon laser (JC-1-excitation). JC-1 green fluorescence (F11) and JC-1 orange fluorescence (F12) were collected with a 530 (± 15) nm and a 575 (± 13) nm band pass filter, respectively. A minimum of 10^4 cells was analyzed (after debris and aggregates elimination) for each sample. Cytometric data were analyzed with Win MDI 2.8 software (developed by Dr J Trotter, Scripps Institute, La Jolla, CA). Gates were set using an F12 vs. F14 cytogram for control cells.

Protein extraction and Western blot analysis. Western blot analysis was performed as previously described (15). Briefly, anti-Bax and anti-Bcl-2 were used at a dilution of 1:200, while anti- β -actin was used at 1:5000 and horseradish-peroxidase-linked secondary antibody at 1:1000. Antibody binding was detected with the ECLTM Western blotting detection reagent kit (Amersham Pharmacia Biotech, Saclay, France) followed by autoradiography (1D Image Analysis Software, Kodak).

Statistical analyses. Data are expressed as the mean \pm SD of three or more separate experiments. Statistical analysis of the data included an overall analysis of variance followed by the posthoc PLSD Fisher's test, using statistical functions in the Statview program (SAS Institute, Cary, NC). A probability of $p < 0.05$ was considered significant.

Results

Effect of UA on caspase activities. The results of caspase-3 activity, at 24 h showed that it was not modified in HaCaT cells compared to the control regardless of UA concentrations

(Fig. 1A). However, after 48 h of treatment, caspase-3 activity was significantly increased at 12.5 and 15 μ M UA (2.9- and 4.7-fold vs. control) (Fig. 1C). In M4Beu cells, caspase-3 activity was significantly increased at as little as 12.5 μ M after 24 h of treatment (1.74- and 2.12-fold vs. control for 12.5 and 15 μ M UA, respectively) (Fig. 1B). Similarly, after 48 h of treatment caspase-3 activity was increased between 12.5 and 15 μ M UA (1.27- and 1.98-fold vs. control, respectively) (Fig. 1D).

In the case of caspase-9, no significant activity was detected in HaCaT cells after 24 h of treatment (Fig. 2A). Caspase-9 activity was significantly increased only at 48 h (1.26- and 1.71-fold vs. control at 12.5 and 15 μ M UA, respectively) (Fig. 2C). For M4Beu cells, caspase-9 activity increased slightly after 24 and 48 h at 15 μ M UA (1.13- and 1.21-fold vs. control, respectively) (Fig. 2B and D).

JC-1/TOTO-3 double staining of $\Delta\psi_m$ by FCM. Having demonstrated caspase-9 activation (e.g. intrinsic pathway triggering) in HaCaT and M4Beu cell lines, we further analyzed $\Delta\psi_m$ evolution. To follow and quantify $\Delta\psi_m$ changes, we performed JC-1/TOTO-3 double staining by FCM (Fig. 3). First, fluorescent probe TOTO-3 separated cells which had maintained membrane integrity from those which had lost it. Second, in viable cells (i.e. TOTO-3⁻) only, JC-1 allowed for the estimation of the percentage of cells with high and low mitochondrial potential. Sub-population positions on cytograms were determined according to a positive control (i.e. oxidative stress following H₂O₂ exposure; Fig. 3B and G). After UA treatment, we observed two cell populations which, due to JC-1 fluorescence shifts from orange to green, indicated a collapse of $\Delta\psi_m$. In HaCaT-treated cells, only a slight drop in mitochondrial potential was seen at 10, 12.5 and 15 μ M UA

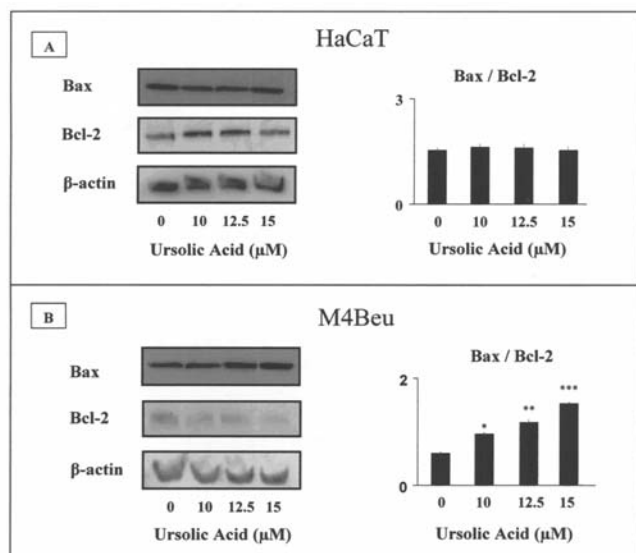


Figure 4. Bax and Bcl-2 protein expression after UA treatment. HaCaT and M4Beu cells were incubated in the presence or absence of UA for 24 h. Bax and Bcl-2 proteins were quantified using β -actin protein as an internal control. Quantification of each band was performed by densitometry analysis software and the results were expressed as the ratio of Bax/Bcl-2 in relative arbitrary units. Results are the mean \pm SD (* p <0.05; ** p <0.01; *** p <0.005) of three separate experiments.

with, respectively, 5.43, 4.48 and 6.27% of the cells having low potential (Fig. 3C-E). In M4Beu cells, UA strongly induced a drop in mitochondrial potential in a dose-dependent way: 17.69% of cells had low potential at 10 μ M, and up to 62.18% had it at 15 μ M (Fig. 3H-J).

Bax and Bcl-2 protein expression. Activation of the mitochondrial intrinsic pathway follows a drop in $\Delta\psi_m$, which is closely regulated by Bcl-2 family members. Hence, we studied the effects of UA treatment on both Bax and Bcl-2 expression, which are the two major regulators of mitochondrial membrane permeabilization. On the one hand, UA-treated HaCaT cells did not show any variation in Bax and/or Bcl-2 expression, which was confirmed by the Bax/Bcl-2 ratio (Fig. 4A). On the other hand, in M4Beu-treated cells Bax expression was significantly increased 1.19-, 1.41- and 1.63-fold vs. control at 10, 12.5 and 15 μ M UA, respectively. Moreover, we concomitantly observed a decrease in Bcl-2 expression of 1.08-, 1.10- and 1.18-fold less vs. control. Finally, our results showed that, in M4Beu cells, UA induced a significant increase in the Bax/Bcl-2 ratio of 1.29-, 1.55- and 1.94-fold vs. control for 10, 12.5 and 15 μ M UA, respectively (Fig. 4B).

Discussion

For the past twenty years, various scientific reports have shown that UA has many beneficial pharmacological effects for human health. Among the most convincing, it has been reported that UA possesses anti-inflammatory, antibacterial, hepatoprotective, anti-tumor and anti-proliferative properties (21). Because of its different biological properties and the fact that UA occurs naturally in a large variety of vegetarian food, this compound is a very interesting anticancer chemopreventive agent (22,23). Furthermore, dietary agents derived from natural sources are considered pharmacologically safe

and can be used in combination with chemotherapeutic agents to enhance their effect at lower doses, thus minimizing chemotherapy-induced toxicity. In previous reports, we postulated that UA could be of interest in the prevention or treatment of skin cancers. In fact, we clearly demonstrated that UA induced apoptosis in HaCaT-derived keratinotic (14) and M4Beu melanoma (15) cell lines. Nevertheless, thorough studies must be carried out to explain the various mechanisms of UA actions with regard to its proapoptotic effects on these cancer cell lines and, particularly, on mitochondria.

Apoptotic cell death involves a cascade of proteolytic events accomplished mainly by a family of cysteine proteases (24) such as caspase-3, the major executioner of apoptosis (25). We demonstrated that UA induces an increase in caspase-3 activity in a dose-dependent manner, associated with a significant but weaker caspase-9 activity, in both HaCaT and M4Beu cells. Indeed it is well established that the activity of initiator caspases is always less than that of executioner ones (25). Caspase inhibitors (Ac-DEVD-CHO and Ac-LEHD-CHO) were used only to ensure the specificity of the catalytic activities studied whatever the experimental conditions. At the same time, we failed to demonstrate any caspase-8 activity (data not shown). As caspase-9 activation is closely linked to a drop in $\Delta\psi_m$ (26), an upstream event that occurs before caspase activation (and more particularly before caspase-9 and caspase-3 activation), we further explored the relative implication of the mitochondrial-apoptotic pathway in UA-treated HaCaT and M4Beu cells.

It is well established that mitochondria play a key role in apoptosis. One critical step is mitochondrial permeability transition pore (PTP) opening, leading to mitochondrial membrane integrity disruption and inner transmembrane proton gradient dissipation (27). PTP opening leads to the release of so-called apoptotic initiation factors that induce downstream apoptotic degradative events. In this manner, mitochondrial membrane permeabilization loss apparently constitutes one major checkpoint leading to cell death. Methods have been developed to estimate mitochondrial transmembrane potential modifications by FCM with cationic lipophilic dyes (28,29). Recently, JC-1 dye has been proposed to more accurately evaluate changes in mitochondrial activity (20,30). JC-1 is selectively incorporated into mitochondria in a monomeric form emitting at 527 nm after excitation at 488 nm with an argon laser. Moreover, depending on the high mitochondrial membrane potential, JC-1 is able to form aggregates emitting at 590 nm. In other words, intact cells with high mitochondrial polarization are indicated by orange fluorescence (JC-1^{high}) due to JC-1 aggregate formation, while apoptotic cells with low mitochondrial polarization (JC-1^{low}) are indicated by the green fluorescence of JC-1 monomers. Thus, a fluorescence shift from orange to green (i.e. $\Delta\psi_m$ collapse) is obtained during mitochondrial apoptotic processes. In addition, TOTO-3 labeling discriminates between two cell subpopulations: cells that maintain cytoplasmic membrane integrity (e.g. TOTO-3⁻) and cells that have lost cytoplasmic membrane integrity (e.g. TOTO-3⁺). Our FCM analyses were calibrated with 1 mM H₂O₂ according to Zuliani *et al* (20). TOTO-3 staining was done in order to perform JC-1 staining on only those cells having intact cytoplasmic membranes (e.g. TOTO-3⁻) (Fig. 3). Moreover, JC-1/TOTO-3 double



SPANDIDOS was recently described as providing a more reliable

ous assessment of the plasma membrane integrity and mitochondrial transmembrane potential occurring during apoptosis (20). As mitochondrial internal membrane potential dissipation is well-defined as an early apoptotic event (31), we decided to study this process after 24 h of UA treatment. Consequently, HaCaT and M4Beu cells were double stained with JC-1/ TOTO-3. Surprisingly, in the case of treated HaCaT cells we observed few cells with low mitochondrial potential (6.27% with 15 μ M) (Fig. 3C-E). For M4Beu cells treated with up to 10 μ M UA, we detected a larger JC-1^{low} sub-population (17.69%). Hence, we clearly demonstrated that UA induced a dose-dependent collapse in M4Beu cells that resulted in approximately 62% of cells having a low mitochondrial membrane potential at 15 μ M UA (Fig. 3H-J).

In the literature, $\Delta\psi$ m collapse has been reported to be under the control of two Bcl-2 family members, Bax and Bcl-2. Bax is responsible for PTP opening while Bcl-2 keeps the PTP closed (32). We detected no variation in Bax or Bcl-2 protein expression in HaCaT cells (Fig. 4A) whereas, in M4Beu cells, we demonstrated that UA increased Bax protein expression in a dose-dependent manner while, at the same time, Bcl-2 protein expression decreased (Fig. 4B). Hence, increasing the Bax/Bcl-2 ratio precipitated PTP opening and the induction of apoptosis through the intrinsic pathway.

These observations lead us to assume that UA-induced apoptotic cell death in M4Beu cells is closely associated with the triggering of the mitochondrial intrinsic pathway.

In the present study, we performed for the first time a comparison of the effects of UA on two different cell lines, M4Beu melanoma cells and HaCaT-derived keratinotic cells. We showed that UA performs a specific action depending on cell type. In effect, our observations lead us to assume that UA-induced apoptotic cell death in M4Beu cells is closely associated to the triggering of the mitochondrial intrinsic pathway while, in HaCaT cells, several lines of evidence suggest that mitochondria are less implicated in UA-induced apoptosis, prompting us to speculate that another apoptotic pathway could be involved.

Acknowledgements

The expenses of this work were defrayed in part by the Conseil Régional du Limousin and by the Ligue National contre le Cancer du Limousin.

References

- Liu J: Oleanolic acid and ursolic acid: research perspectives. *J Ethnopharmacol* 100: 92-94, 2005.
- Rona C, Vailati F and Berardesca E: The cosmetic treatment of wrinkles. *J Cosmet Dermatol* 3: 26-34, 2004.
- Yarosh DB, Both D and Brown D: Liposomal ursolic acid (merotaine) increases ceramides and collagen in human skin. *Horm Res* 54: 318-321, 2000.
- Soo Lee Y, Jin DQ, Beak SM, Lee ES and Kim JA: Inhibition of ultraviolet-A-modulated signaling pathways by asiatic acid and ursolic acid in HaCaT human keratinocytes. *Eur J Pharmacol* 476: 173-178, 2003.
- Huang MT, Ho CT, Wang ZY, *et al*: Inhibition of skin tumorigenesis by rosemary and its constituents carnosol and ursolic acid. *Cancer Res* 54: 701-708, 1994.
- Tokuda H, Ohigashi H, Koshimizu K and Ito Y: Inhibitory effects of ursolic and oleanolic acid on skin tumor promotion by 12-O-tetradecanoylphorbol-13-acetate. *Cancer Lett* 33: 279-285, 1986.
- Baek JH, Lee YS, Kang CM, Kim JA, Kwon KS, Son HC and Kim KW: Intracellular Ca²⁺ release mediates ursolic acid-induced apoptosis in human leukemic HL-60 cells. *Int J Cancer* 73: 725-728, 1997.
- Lauthier F, Taillet L, Trouillas P, Delage C and Simon A: Ursolic acid triggers calcium-dependent apoptosis in human Daudi cells. *Anticancer Drugs* 11: 737-745, 2000.
- Hollosy F, Idei M, Csorba G, *et al*: Activation of caspase-3 protease during the process of ursolic acid and its derivative-induced apoptosis. *Anticancer Res* 21: 3485-3491, 2001.
- Hsu YL, Kuo PL and Lin CC: Proliferative inhibition, cell-cycle dysregulation, and induction of apoptosis by ursolic acid in human non-small cell lung cancer A549 cells. *Life Sci* 75: 2303-2316, 2004.
- Satomi Y, Nishino H and Shibata S: Glycyrrhetic acid and related compounds induce G1 arrest and apoptosis in human hepatocellular carcinoma HepG2. *Anticancer Res* 25: 4043-4047, 2005.
- Achiwa Y, Hasegawa K, Komiya T and Udagawa Y: Ursolic acid induces Bax-dependent apoptosis through the caspase-3 pathway in endometrial cancer SNG-II cells. *Oncol Rep* 13: 51-57, 2005.
- Achiwa Y, Hasegawa K and Udagawa Y: Molecular mechanism of ursolic acid induced apoptosis in poorly differentiated endometrial cancer HEC108 cells. *Oncol Rep* 14: 507-512, 2005.
- Harmand PO, Duval R, Liagre B, Jayat-Vignoles C, Beneytout JL, Delage C and Simon A: Ursolic acid induces apoptosis through caspase-3 activation and cell cycle arrest in HaCat cells. *Int J Oncol* 23: 105-112, 2003.
- Harmand PO, Duval R, Delage C and Simon A: Ursolic acid induces apoptosis through mitochondrial intrinsic pathway and caspase-3 activation in M4Beu melanoma cells. *Int J Cancer* 114: 1-11, 2005.
- Roy S and Nicholson DW: Cross-talk in cell death signalling. *J Exp Med* 192: 21-26, 2000.
- Stennicke HR, Jurgensmeier JM, Shin H, *et al*: Pro-caspase-3 is a major physiologic target of caspase-8. *J Biol Chem* 273: 27084-27090, 1998.
- Antonsson B and Martinou JC: The Bcl-2 protein family. *Exp Cell Res* 256: 50-57, 2000.
- Borner C: The Bcl-2 protein family: sensors and checkpoints for life-or-death decisions. *Mol Immunol* 39: 615-647, 2003.
- Zuliani T, Duval R, Jayat C, Schnebert S, Andre P, Dumas M and Ratinaud MH: Sensitive and reliable JC-1 and TOTO-3 double staining to assess mitochondrial transmembrane potential and plasma membrane integrity: interest for cell death investigations. *Cytometry* 54: 100-108, 2003.
- Liu J: Pharmacology of oleanolic acid and ursolic acid. *J Ethnopharmacol* 49: 57-68, 1995.
- Novotny L, Vachalkova A and Biggs D: Ursolic acid: an anti-tumorigenic and chemopreventive activity (Minireview). *Neoplasma* 48: 241-246, 2001.
- Ovesna Z, Vachalkova A, Horvathova K and Tothova D: Pentacyclic triterpenoic acids: new chemoprotective compounds (Minireview). *Neoplasma* 51: 327-333, 2004.
- Alnemri ES, Livingston DJ, Nicholson DW, Salvesen G, Thornberry NA, Wong WW and Yuan J: Human ICE/CED-3 protease nomenclature. *Cell* 87: 171, 1996.
- Earnshaw WC, Martins LM and Kaufmann SH: Mammalian caspases: structure, activation, substrates, and functions during apoptosis. *Annu Rev Biochem* 68: 383-424, 1999.
- Loeffler M and Kroemer G: The mitochondrion in cell death control: certainties and incognita. *Exp Cell Res* 256: 19-26, 2000.
- Reed JC, Jurgensmeier JM and Matsuyama S: Bcl-2 family proteins and mitochondria. *Biochim Biophys Acta* 1366: 127-137, 1998.
- Darzynkiewicz Z, Traganos F, Staiano-Coico L, Kapuscinski J and Melamed MR: Interaction of rhodamine 123 with living cells studied by flow cytometry. *Cancer Res* 42: 799-806, 1982.
- Shapiro HM: Cell membrane potential analysis. *Methods Cell Biol* 41: 121-133, 1994.
- Cossarizza A, Baccarani-Conti M, Kalashnikova G and Franceschi C: A new method for the cytofluorimetric analysis of mitochondrial membrane potential using the J-aggregate forming lipophilic cation 5,5',6,6'-tetrachloro-1,1',3,3'-tetraethylbenzimidazolcarbocyanine iodide (JC-1). *Biochem Biophys Res Commun* 197: 40-45, 1993.
- Kroemer G and Reed JC: Mitochondrial control of cell death. *Nat Med* 6: 513-519, 2000.
- Kroemer G: Mitochondrial control of apoptosis. *Bull Acad Natl Med* 185: 1135-1143, 2001.